RSC Advances

RSC Advances

www.rsc.org/advances

ROYAL SOCIETY OF CHEMISTRY

www.rsc.org/advances

Electronic structure and optical properties of silicon nitride adsorbed by rare earths are explored by density functional theory.
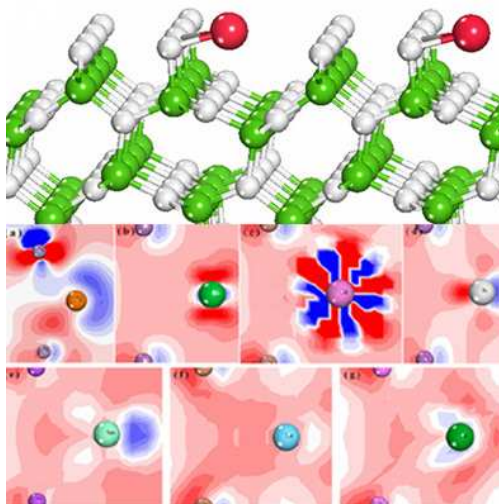
ARTICLE TYPE

Effects of rare earth adsorption on electronic structure and optical properties in β-Si₃N₄ ceramics from first principles

Yin Wei,[a] Hongjie Wang,*[a] Xuefeng Lu,[a] Jiangbo Wen,[a] Min Niu,[a] Xingyu Fan,[a] and Shuhai Jia*[b]

Electronic structure and optical properties of silicon nitride adsorbed by rare earths are explored by density functional theory. The fully relaxed structural parameters are found to be in good accordance with experimental data. Covalent character of polar covalent bonds by rare earth adsorption is in the order of Gd, Yb, Sc, Sm, La and Lu, which is verified by population values. Gd, 10 Yb, Sc and La adsorption systems may exhibit longer life in applications as dielectric materials in the low energy regions due to low static dielectric constant and loss, as well as transparent type characteristic exhibited in visible regions.

Capturing the atomic level influences of rare earth (RE) sintering additives in the resulting crystalline/amorphous interfacial 15 configuration has stirred numerous interests due to it is the critical element that controls most of the materials' characteristics, most significantly the mechanical properties, which are dependent on the local chemical composition, atomic structure, and bonding characteristics, in silicon nitride 20 ceramics.[1,2] Some of RE species can segregate to grain surfaces and adsorb there according to the chemical driving force and competition with Si atoms.[3-6] After densification, these grains-boundary phases are known to greatly affect the resulting microstructure and properties of ceramics, and it is thus important 25 to understand the underlying mechanism and effects of adsorption at internal interface, as well as the reasons for displayed discriminations among the RE series. Simultaneously, it opens a window in application fields of microelectric and aerospace by taking insight into the dielectric and optical properties of the β-30 Si₃N₄ ceramics with various RE adsorption.

Considerable sweats have been swallowed to see through clearly bonding state and mechanism at amorphous/crystalline interface for both experimental and theoretical studies. It is well established that ultimate ceramics structure consists of elongated 35 Si₃N₄ matrix grains embedded in an intergranular, typically amorphous, oxide phase resembling that of whisker enhanced ceramics, which are sensitive to the types of cations of the selected sintering additions.[7,8] Experiments suggest that growth on the prism planes is reaction rate limited accompanying the 40 segregation of rare-earth atoms and thus, relatively slow compared to that in the basal planes, which belongs to diffusion control and is rapid. The resulted grains with large aspect ratios

[a] *State Key Laboratory for Mechanical Behavior of Materials, Xi'an Jiaotong University, Xi'an, 710049, China*

45 *E-mail: hjwang@mail.xjtu.edu.cn; Fax:029-82663453; Tel: 029-82667942*

[b] *School of Mechanical Engineering, Xi'an Jiaotong University, Xi'an 710049, China*

E-mail: shjia@mail.xjtu.edu.cn; Fax:029-82668556; Tel: 029-82668556

are obtained.[9-12] Theoretically, the grain growth is found to 50 originate from the site competition between REs and Si for bonding at β-Si₃N₄ interfaces, as well as stereochemical bonding factors.[13,14] The previous investigations of the interfaces have focused on the segregation and absorption sites of rare earths in the intergranular phase. What is needed in engineering controls is 55 a simple measure of the relative preference of dopant cations for bonding at interfaces. However, the information about the electronic density difference, bond nature and mechanical properties after adsorption is absent. Since principles of micrometer-scale structural design are generally employed to 60 enhance the mechanical properties of ceramics, this work represents a step towards the atomic-level structural engineering control required for the next generation of ceramics. Our objective is the investigation of bonding characteristics of RE with N sites for a larger selection of the oxide sintering additions 65 and to complete previous researches by analyzing their electronic configuration and optical property discrepancy.

In this paper, we capture the electronic density difference, bond nature and optical properties after adsorption using first principles calculations with regard to GGA-PW91 equations, motivated by 70 the fact that these nanoscale structures effectively control macroscopic ceramic behaviour, in which new functional parameters are obtained by the known parameters or other accurate theoretical help. Simultaneously, the exchange-correlation energy is suitable for calculating the binding energy 75 and elastic constants and not suitable for calculating the surface energy and oxides properties. Fig.1 demonstrates the calculated surface configurations of β-Si₃N₄ crystal structure with RE adsorption. In the basic unit, the three outer layers of atoms can be optimized and relaxed, and the rest of the inner atoms are 80 fixed unchanged. Atoms in adjacent unit along the y direction (see Fig.1(b)) are separated by at least 10 Å so as to minimize any spurious interaction between units. The initial cell sizes are a=5.822Å, b=7.607Å, c= 16.258Å. Brillouin zone integration is performed employing a discrete 4×4×10 Monkhorst-Pack k point
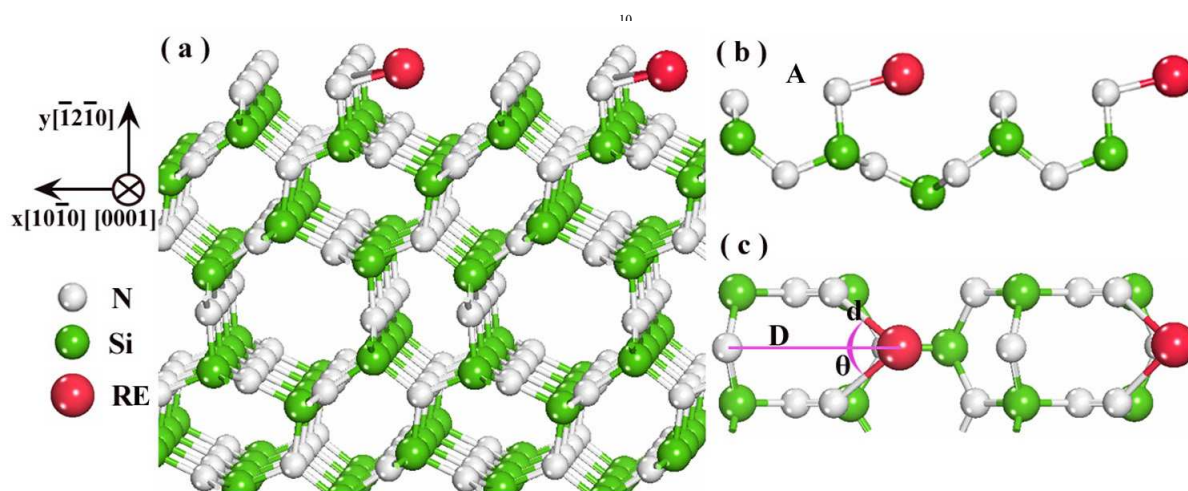
Fig.1 The surface configurations of β-Si$_3$N$_4$ crystal structure with RE adsorption. N: white atoms; Si: green atoms; RE: red atoms. (a) atomic cluster model viewed slightly off normal to the basal plane. (b) the local amplification model surface. (c) top view of atom cluster model of surface.

sampling. We use plane wave basis sets with a kinetic energy cutoff of 480 eV, in conjunction with ultrasoft pseudopotentials for describing the ion-electron interaction. But when optical properties are calculated, norm conserving pseudopotentials are preferable. The pseudopotentials involves the following atomic orbitals in their respective valences: Si(3s2, 3p2), N(2s2, 2p2), Sc(3s2, 3p6, 3d1, 4s2), La(5s2, 5p6, 5d1, 6s2), Sm(4f6, 5s2, 5p6, 6s2), Gd(4f7, 5s2, 5p6, 5d1, 6s2), Yb(4f14, 5s2, 5p6, 6s2), Lu(4f14, 5p6, 5d1, 6s2).

To obtain the stable adsorption systems, we firstly conduct the optimization by relaxing both the internal coordinates and the lattice constants by means of calculating the ab initio forces on the ions with the Born-Oppenheimer approximation, until the absolute values of the forces are converged to less than 0.01eV/Å. Calculated equilibrium adsorption sites in the cluster are illustrated in Fig.2 and relevant parameters, such as covalent radius (CR), total energy (TE), band gap (BG), band angle (BA), D and d, are listed in Table 1. It is found that all the adsorption sites are located near A point in Fig.1 (b), which is similar to that reported by Gayle.[14] The calculated TE values predict that Yb adsorption system is more stable than other
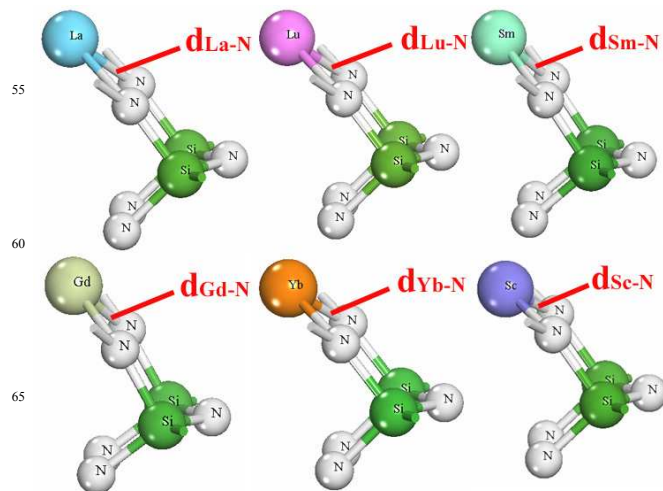

Fig.2 Surface configuration patterns of RE atoms adsorbed on the prismatic plane.

Table 1 The covalent radius and calculated total energy (TE), band gap (BG), band angle (BA), D and d values. Theoretical and experimental values come from Refs. 14 and 15.

RE	CR(Å)	TE/eV	BG/eV	BA(θ)/degree	D$_{RE-N}$/Å	Expt. D$_{RE-N}$/Å	Theor. D$_{RE-N}$/Å	d$_{RE-N}$/Å
Sc	1.44	-2.9587×10^3	0.498	99.229	2.10	---	---	1.97
Lu	1.56	-7.4502×10^3	0.154	83.503	2.38	2.20[±0.2]	2.11	2.25
Gd	1.62	-4.7163×10^3	0.100	89.440	2.33	2.33[±0.2]	2.21	2.13
Sm	1.62	-3.8808×10^3	0.104	87.404	2.38	---	---	2.17
La	1.69	-2.5417×10^3	0.110	79.772	2.41	2.40[±0.3]	2.29	2.34
Yb	1.74	-8.0741×10^3	0.102	90.671	2.28	---	---	2.12

systems. The BG decreases gradually in the order of Sc>Lu>La>Sm>Yb>Gd, indicating that the distance between the valence band and the conduction band becomes narrowest in Ga adsorption system. The D values (the distance of RE with N atom in one unit), in experimental measurements and theoretical calculations, are obtained by the Pythagorean Theorem from reported values, which are used to compare with the calculated D values in this present work. With the reported theoretical values, the calculated values have a maximum deviation of 0.27 Å. With the experimental values, the calculated values are within the experimental errors reported in literature and hence are reliable. The calculated d_{RE-N} values (the bond length of RE and N atoms) decrease in the order of La>Lu>Sm>Ga>Yb>Sc, which is in accordance with the configuration exhibited in Fig.2. This may be due to the two reasons that atomic radius and electronegativity. The atomic radius is in the order of La>Sm>Gd>Yb>Lu>Sc, which is in accordance with the order of the d values except Lu element. The reason is attributed to higher electronegativity of Lu element, leading to the larger bond length by polarization action.

For the purpose of clarifying the nature of the bonds that a RE forms with N atoms, description of adsorption state is illustrated in Fig.3, where charge density difference[16,17] (the change in charge density owing to RE adsorption bond) is shown. Blue and red parts displayed in maps mean the electron deficiency and enrichment, respectively. The changes in electron density are obvious when the RE atoms adsorb on prismatic plane. Compared to the original system, blue area around Sm atom decreases, i.e. electron deficiency weakens, indicating that covalent character of adsorption bond reduces. Meanwhile, blue areas around La and Lu atoms almost disappear, stating clearly that the great decrease in electron deficiency and it illustrates that covalent character of adsorption bond attenuates dramatically and the covalent-ionic transition occurs. For the systems of Yb, Gd and Sc adsorption,

except the reduction in the blue area, one can see that the red area is present, indicating that electron enrichment increases around RE atoms accompanying the uneven distribution of electron cloud, resulting in the lighter reducing amplitude of electron deficiency compared to the first three RE elements. This makes known that the Yb, Gd and Sc adsorption bonds keep some covalent character. In the cases, the degree of inhomogeneous distribution of electron cloud in Gd adsorbed system is larger than that in other two systems, revealing that polar covalent bond with N atom formed by Gd adsorption is stronger in all three systems, and the next element is Yb. Combined with the above analysis, covalent caused by RE adsorption is in the order of Gd>Yb>Sc>Sm>(La, Lu).

To verify the deductive results, population values are calculated with regard to various adsorption systems. Distributions of electron charges in terms of different atoms can be illustrated by the atomic population analysis. Owing to atomic charges are sensitive to used set, the calculated population values has no absolute meaning but only relative one. In the majority of methods, Milliken population analysis is extensively employed because it provides a way of evaluating partial atomic charges from calculations conducted by the computational chemistry methods, and particularly those based on the linear combination of atomic orbital method, and are routinely used as variables in linear regression procedures. Simultaneously, the overlap degree of the electron cloud of two bonding atoms, as well as colavent

Table 2 The calculated population values of bonds by RE adsorption

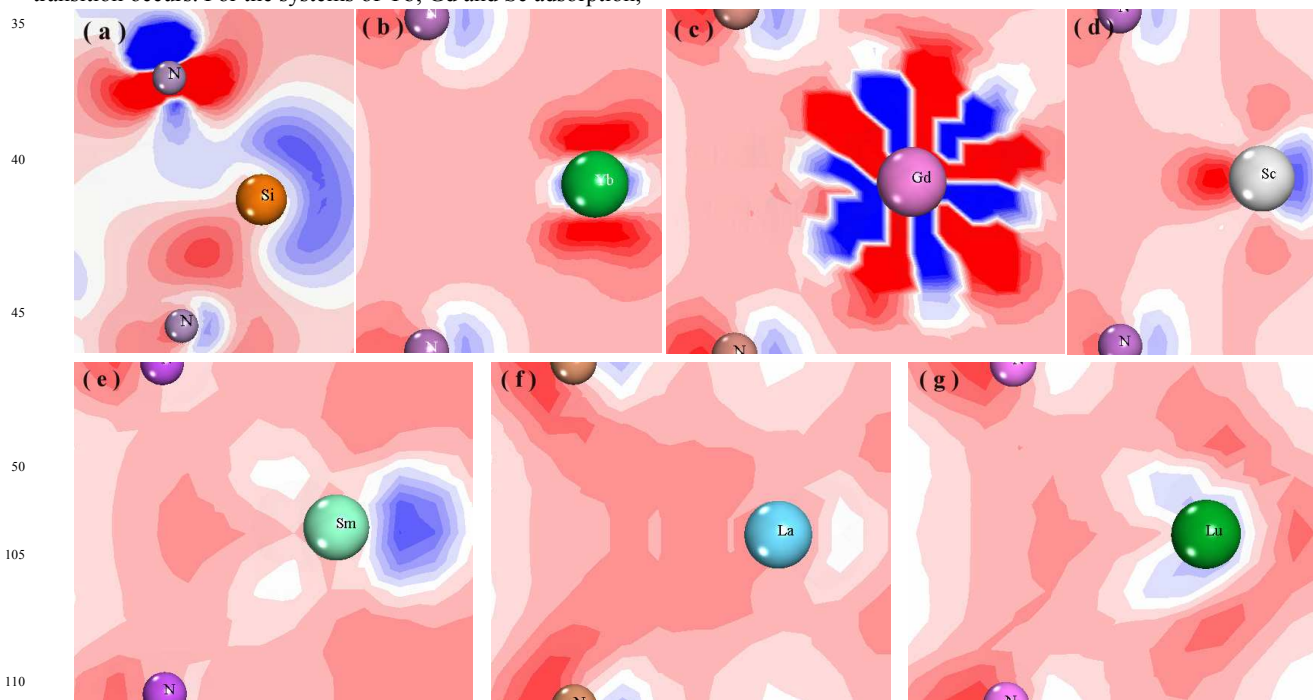|	Gd	Yb	Sc	Sm	La	Lu
RE-N	0.25	0.20	0.19	0.17	0.14	-4.73

Fig.3 Charge density difference maps of RE adsorption systems character of polar covalent bonds. The figures are projected along cylindrical surfaces (cutting along (0001)surface).

and ionic nature of a chemical bond, may be explained by the bond population. Chemically, the positive and negative Mulliken population values correspond to a bond and an anti-bonding character, respectively. The highest and lowest values for the bond population represent the strong covalent and ionic chemical bond nature, respectively. Table 2 shows the calculated population distribution results. It is found that the values decrease gradually in the order of Gd>Yb>Sc>Sm>La>Lu, which is in agreement with the analysis results of charge density difference.

Optical properties are of essential importance due to they not only embody the occupied and unoccupied parts of the electronic structure but also convey the information about the characteristic of bands. The optical properties may be obtained from the dielectric function $\varepsilon(\omega) = \varepsilon_1(\omega) + i\varepsilon_2(\omega)$, which is calculated from the momentum matrix elements between the occupied and unoccupied wave functions by means of Ehrenreich and Cohen.[18] Fig.4 illustrates the dielectric constant of photon energy changes for various RE adsorption systems. It can be seen that dielectric
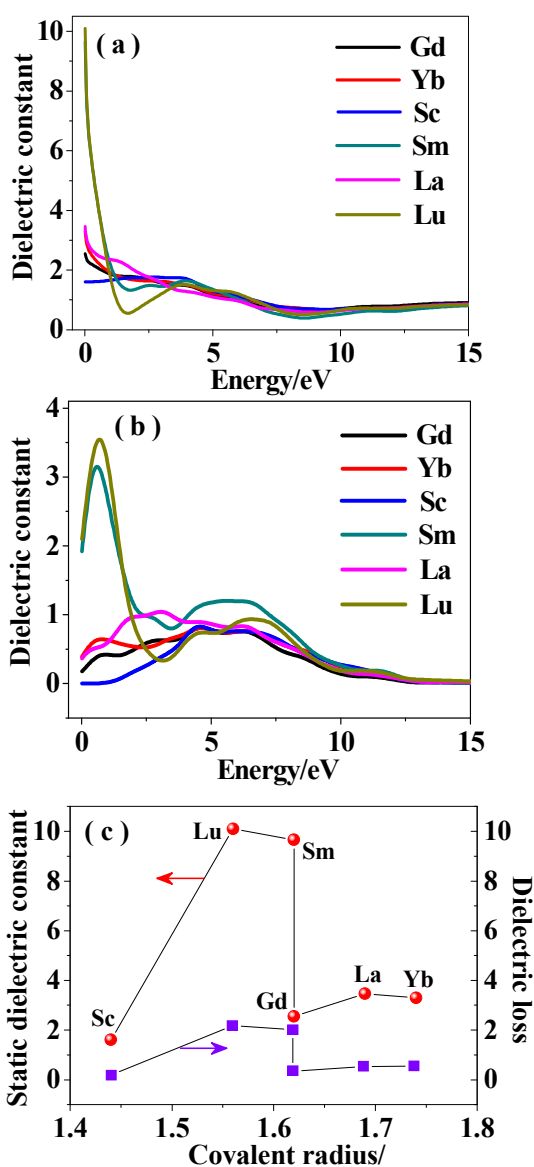
constant decreases gradually with photon energy increasing and keeps steady finally. The static dielectric constants located in the low energy region are 10.05 and 9.76, respectively, for Lu and Sm adsorption systems, larger than that of the other four systems (see Fig.4a), caused by higher bond dipole moment and polarizability. Correspondingly, the change is similar to that of imaginary part shown in Fig.4b. In summary, with the increasing of covalent radius, the static dielectric constant and dielectric loss increase firstly and then decrease and finally become unchanged (see Fig.4c). This reveals that Gd, Yb, Sc and La adsorption systems can exhibit longer life in applications as dielectric materials in the low energy regions due to low static dielectric constant and loss. The Lu- and Sm-adsorbed cases have plasma response.

Fig.5 shows the adsorption coefficient and reflection spectrum curves of various RE adsorption systems. One can see that for Sm, Lu, La, Sc, Yb and Gd adsorptions, the adsorption coefficients come to the maximum values at 166, 165, 186, 165, 174 and 182 nm, respectively and simultaneously for Gd, Sm and Yb adsorption, the second peak values are present at 47, 43 and 43 nm, respectively (see Fig.5a), indicating that in the ultraviolet regions the adsorption systems may emerge "Barrier Type" properties. In the visible regions that the wavelength is in the range of 390 to 780 nm, the adsorption systems represent lower adsorption coefficients, explaining that all the systems except Lu and Sm adsorption may exhibit "Transparent Type" characteristic. From the reflection spectrums (see Fig.5b), it is found that the

Fig.4 Dielectric constant curves of various RE adsorption systems. (a) real part; (b) imaginary part; (c) covalent radius dependence.
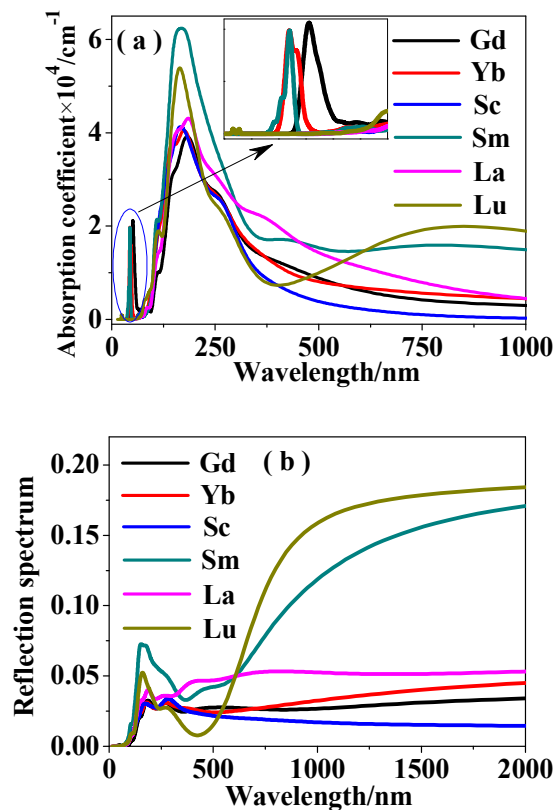

Fig.5 Adsorption coefficient and reflection spectrum curves of various RE adsorption systems

values of Lu and Sm adsorption systems are higher than that of the other four systems in visible regions, showing that part energy loss occurs. Combined with the analysis results of Fig.5a, it is concluded that light spreads more easily in the systems of Gd, Yb, Sc and La adsorption ones.

Conclusions

In summary, we conduct the study on the first principles of electronic structure and optical properties of rare earth adsorption at β-Si$_3$N$_4$ interface. The fully relaxed structural parameters are found to be in good accordance with experimental data. Charge density difference results illustrate that covalent character of polar covalent bonds by RE adsorption is in the order of Gd>Yb>Sc>Sm>(La, Lu), which is verified by calculated population values. Gd, Yb, Sc and La adsorption systems may exhibit longer life in applications as dielectric materials in the low energy regions due to low static dielectric constant and loss, as well as "Transparent Type" characteristic exhibited in visible regions.

Acknowledgements

Notes and references

1 Y. Jiang, Y. Ma and S. H. Garfalini, *Acta Mater.,* 2014, **66**, 284.
2 G. S. Painter and P. F. Becher, *J. Am. Ceram. Soc.,* 2002, **85**, 65.
3 P. F. Becher, G. S. Painter, N. Shibata, R. L. Satet, M. J. Hoffmann and S. J. Pennycook, *Mater. Sci. Eng. A,* 2006, **422**, 85.
4 W. Walkosz, J. C. Idrobo, R. F. Klie, and S. Ogut, *Phys. Rev. B,* 2008, **78**, 165322.
5 X. F. Lu, M. Chen, L. Fan, C. Wang, H. J. Wang, and G. J. Qiao, *Appl. Phys. Lett.,* 2013, **102**, 031907.
6 G. S. Painter and P. F. Becher, *Phys. Rev. B,* 2002, **65**, 064113.
7 J.C. Idrodo, M. P. Oxley, W. Walkosz, R. F. Klie, S. Ogut, B. Mikijelj, S. J. Pennycook, and S. T. Pantelides, *Appl. Phys. Lett.,* 2009, **95**, 164101.
8 M. Chang, Y. Ju, J. Lee, S. Jung, H. Choi, M. Jo, S. Jeon, and H. Hwang, *Appl. Phys. Lett.,* 2008, **93**, 022101.
9 Naoya Shibata, Stephen J. Pennycook, Tim R. Gosnell, Gayle S. Painter, William A. Shelton and Paul F. Becher. *Nature,* 2004, **428**, 730.
10 A. Ziegler, J. C. Idrobo, M. K. Cinibulk, C. Kisielowski. *Science,* 2004, **306**, 1768.
11 N. Shibata, G. S. Painter, R. L. Satet, M. J. Hoffmann, S. J. Pennycook, and P. F. Becher. *Phys. Rev. B,* 2005, **72**, 140101.
12 Naoya Shibata, Gayle S. Painter, Paul F. Becher, and Stephen J. Pennycook. *Appl. Phys. Lett.,* 2006, **89**, 051908.
13 G. S. Painter, P. F. Becher, W. A. Shelton, R. L. Staet, and M. J. Hoffmann. *Phys. Rev. B,* 2004, **70**, 144108.
14 Gayle S. Painter, Frank W. Averill, Paul F. Becher, Naoye Shibata, Klaus van Benthem, and Stephen J. Pennycook. *Phys. Rev. B,* 2008, **78**, 214206.
15 G. B. Winkelmann, C. Dwyer, T. S. Hudson, D. Nguyen-Manh, M. Doblinger, R.L. Satet, M.J. Hoffmann, and D. J. H. Cockayne. *Philos. Mag. Lett.,* 2004, **84**, 755.
16 X. F. Lu, P. Q. La, X. Guo, Y. P. Wei, X. L. Nan and L. He. *Comp. Mater. Sci.,* 2013, **79**,174.
17 F. F. Zhou, J. Han, R. R. Liu, P. Li and H.Y. Zhang. *Comput. Theor. Chem.,* 2014, **1044**, 80.
18 S. Saha, T. P. Sinha and A. Mookerjee. *Phys. Rev. B.* 2000, **62B**, 8828.